1975-12

Investigation of gravitational effects on a variable conductance heat pipe utilizing liquid crystal thermography

Batts, William Henry

Monterey, California. Naval Postgraduate School

INVESTIGATION OF GRAVITATIONAL EFFECTS ON A VARIABLE CONDUCTANCE HEAT PIPE UTILIZING LIQUID CRYSTAL THERMOGRAPHY

William Henry Batts

NAVAL POSTGRADUATE SCHOOL
Monterey, California

THESIS

INVESTIGATION OF GRAVITATIONAL EFFECTS
ON A VARIABLE CONDUCTANCE HEAT PIPE
UTILIZING LIQUID CRYSTAL THERMOGRAPHY

by

William Henry Batts, Jr.

December 1975

Thesis Advisor: Matthew Kelleher

UNCLASSIFIED

SECURITY CLASSIFICATION OF THIS PAGE (When Data Entered)

REPORT DOCUMENTATION PAGE		READ INSTRUCTIONS BEFORE COMPLETING FORM
1. REPORT NUMBER	2. GOVT ACCESSION NO.	3. RECIPIENT'S CATALOG NUMBER
4. TITLE (and Subtitle) Investigation of Gravitational Effects on a Variable Conductance Heat Pipe Utilizing Liquid Crystal Thermography		5. TYPE OF REPORT & PERIOD COVERED Master's Thesis; December 1975
		6. PERFORMING ORG. REPORT NUMBER
7. AUTHOR(s) William Henry Batts, Jr.		8. CONTRACT OR GRANT NUMBER(s)
9. PERFORMING ORGANIZATION NAME AND ADDRESS Naval Postgraduate School Monterey, California 93940		10. PROGRAM ELEMENT, PROJECT, TASK AREA & WORK UNIT NUMBERS
11. CONTROLLING OFFICE NAME AND ADDRESS Naval Postgraduate School Monterey, California 93940		12. REPORT DATE December 1975
		13. NUMBER OF PAGES 53
14. MONITORING AGENCY NAME & ADDRESS(if different from Controlling Office) Naval Postgraduate School Monterey, California 93940		15. SECURITY CLASS. (of this report) Unclassified
		15a. DECLASSIFICATION/DOWNGRADING SCHEDULE

16. DISTRIBUTION STATEMENT (of this Report)

Approved for public release; distribution unlimited.

17. DISTRIBUTION STATEMENT (of the abstract entered in Block 20, if different from Report)

18. SUPPLEMENTARY NOTES

19. KEY WORDS (Continue on reverse side if necessary and identify by block number)

20. ABSTRACT (Continue on reverse side if necessary and identify by block number)

Observations were made of the operation of a gas loaded, variable conductance heat pipe two inches in diameter and sixty inches long. The heat pipe was operated in the horizontal and vertical positions while input power was varied from twenty five to one hundred fifty watts. Liquid crystal thermographic techniques were used to observe the temperature gradients existing when non-condensible gases both heavier and lighter than the

DD FORM 1 JAN 73 1473 EDITION OF 1 NOV 65 IS OBSOLETE
S/N 0102-014-6601 |
(Page 1)

SECURITY CLASSIFICATION OF THIS PAGE (When Data Entered)

working fluid had been introduced. Methanol was used as the working fluid; krypton and helium were the non-condensible gases. Isothermal maps, photographs of liquid crystal displays, and summarized temperature data for the various operating conditions are presented.

Investigation of Gravitational Effects on a Variable Conductance Heat Pipe Utilizing Liquid Crystal Thermography

by

William Henry Batts, Jr.
Commander, United States Navy
B.S., United States Naval Academy, 1959

Submitted in partial fulfillment of the
requirements for the degree of

MASTER OF SCIENCE IN MECHANICAL ENGINEERING

from the

NAVAL POSTGRADUATE SCHOOL

December 1975

ABSTRACT

Observations were made of the operation of a gas loaded, variable conductance heat pipe two inches in diameter and sixty inches long. The heat pipe was operated in the horizontal and vertical positions while input power was varied from twenty five to one hundred fifty watts. Liquid crystal thermographic techniques were used to observe the temperature gradients existing when non-condensible gases both heavier and lighter than the working fluid had been introduced. Methanol was used as the working fluid; krypton and helium were the non-condensible gases. Isothermal maps, photographs of liquid crystal displays, and summarized temperature data for the various operating conditions are presented.

TABLE OF CONTENTS

LIST OF TABLES

LIST OF FIGURES

I. INTRODUCTION

The heat pipe is a very efficient heat transfer device. In its simplest form it is a closed cylinder containing a wick and a condensing/evaporating fluid. There are no moving parts. The wick can be any of several materials and configurations; the essential requirement is that it be capable of moving the working fluid by capillary pumping action. Many geometric configurations of the basic pipe are possible.

A thorough presentation on the theory and design of heat pipes can be found in Marcus [Ref. 1]. This report is particularly concerned with variable conductance heat pipes and includes an extensive bibliography on the subject.

In operation, heat from a source is absorbed by the pipe, evaporating the working fluid. The vapor travels along the pipe to the condenser section where heat is rejected to a sink and the vapor is condensed. The condensate is returned to the evaporator section through the wick by capillary pumping. Due to the phase changes of the working fluid occurring along its length, the basic heat pipe operates at essentially isothermal conditions.

One drawback to this simple system is that, given a constant sink temperature, the heat transfer rate can be increased only by raising the operating temperature of the heat pipe. This is not desirable if the goal is to maintain a constant source temperature.

The gas-loaded variable conductance heat pipe provides a partial solution to this problem. A non-condensible gas is introduced along with the working fluid. During operation the working fluid behaves as described above; however, the non-condensible gas migrates to the condenser end where it forms a plug. This effectively reduces the condenser length and, therefore, the condenser heat transfer area. As the heat transfer rate into the evaporator increases, the temperature and partial pressure of the working fluid increase, compressing the plug of non-condensible gas. The effective condenser heat transfer area is increased, thus modifying and reducing the system temperature rise. This concept of variable conductance is shown graphically in Fig. 1, which is a partial plot of data presented in Appendix A. The addition of the helium gas caused a decrease in the slope of the curve; the slope is a measure of the conductance.

The simplest model for examining the behavior of a gas-loaded heat pipe uses the flat front theory proposed by Bienert [Ref. 2]. This model (see Fig. 2) is based on the following assumptions [Ref. 1]: steady state operation, a flat interface between vapor and gas regions, no axial conduction, heat transfer per unit area of condenser proportional to the temperature difference between vapor and sink, uniform pressure distribution, and ideal behavior of the vapor-gas mixture. Although this model allows some vapor in the gas section (at sink temperature conditions), it is assumed that there is no gas in the vapor section. Experimental results have shown

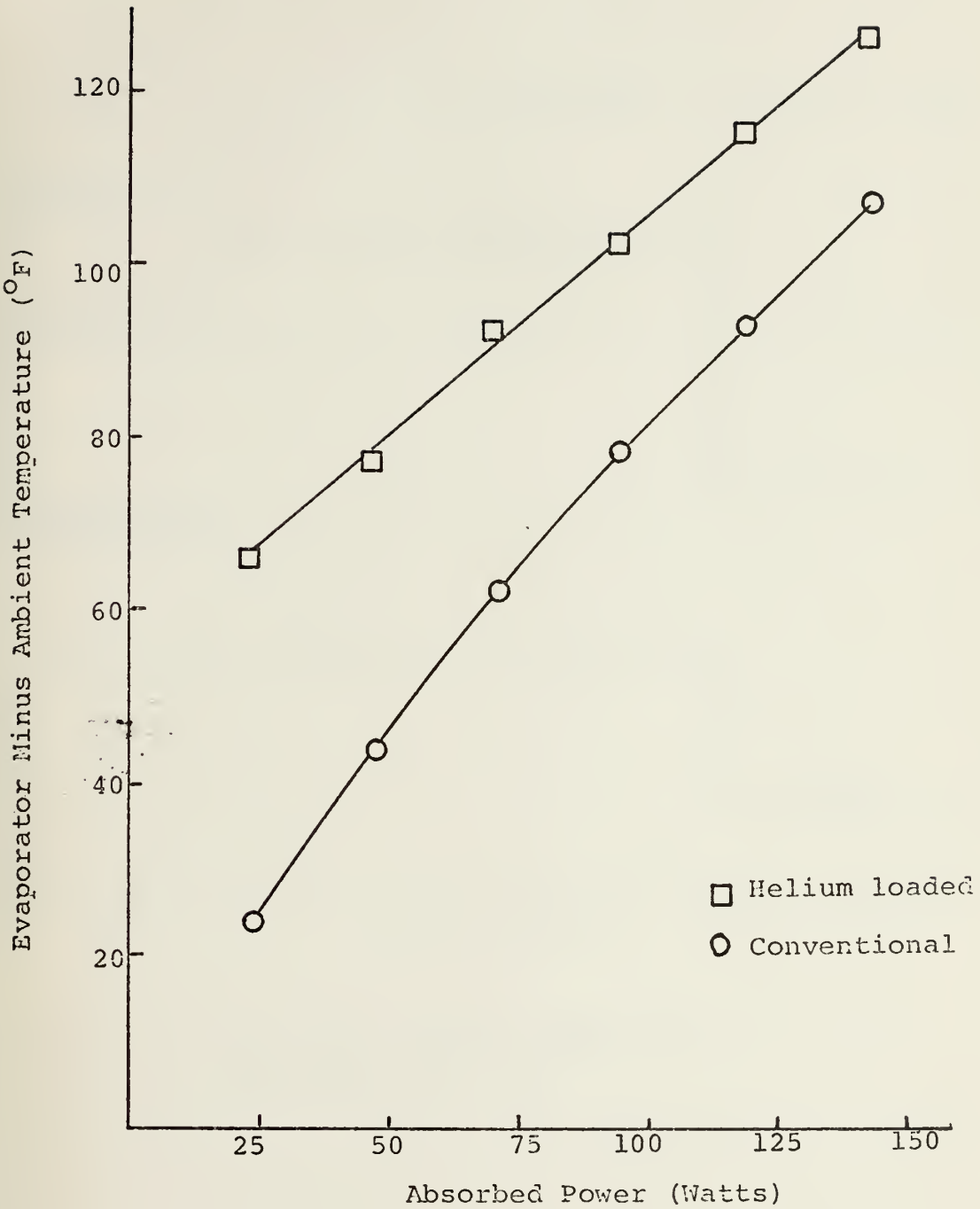

Figure 1. Evaporator Minus Ambient Temperature vs. Absorbed Power

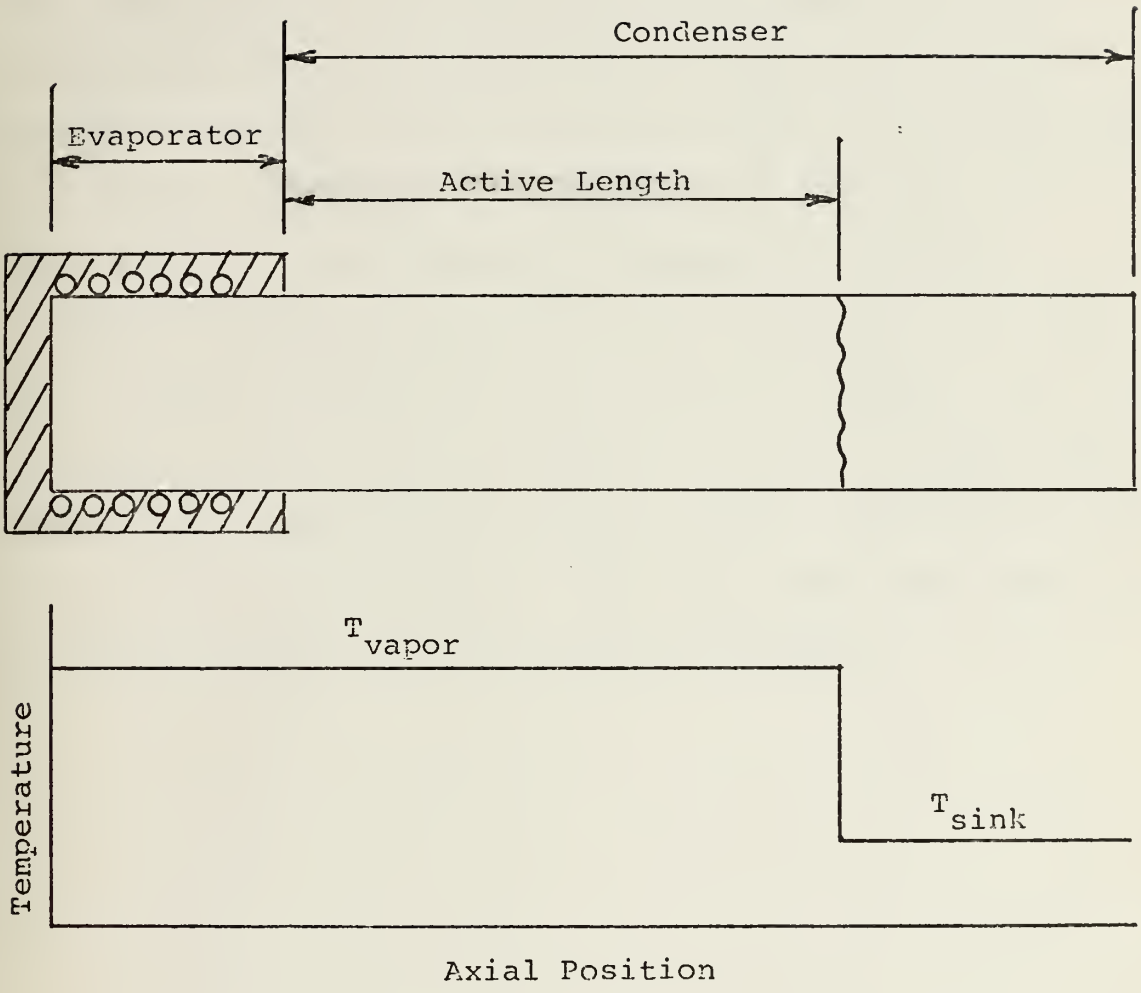

Figure 2. Flat Front Theory Model of a Gas Loaded Heat Pipe

this model to be inaccurate, primarily because it neglects axial conduction and diffusion [Ref. 1].

A more realistic explanation is provided by the diffuse front theory as presented by Marcus [Ref. 1]. The diffuse front theory does treat effects of axial conduction and binary mass diffusion between the vapor and gas. Computer parametric studies by Marcus indicated that axial conduction had a significant effect on spreading the vapor-gas front. The influence of mass diffusion appeared to be minimal.

Possibly because much of the early work with heat pipes has been done in connection with the space program, the effects of gravity have not been considered. Naydan's results [Ref. 3] indicate that gravitational effects may be significant in the case of a low length/diameter ratio heat pipe using vapor and gas of appreciably different molecular weights.

II. OBJECTIVE

The objective of this research was to continue the investigation of gravitational effects on the operating characteristics of a variable conductance heat pipe. A heat pipe with a length/diameter ratio of approximately thirty was operated at various power levels when loaded with different concentrations of gases with molecular weights both greater and less than that of the working fluid. Operating in both vertical and horizontal positions, liquid crystal thermographic techniques were used to detect system isotherms. It was expected that this data would provide additional insight into the nature and orientation of the vapor-gas interface.

III. EXPERIMENTAL APPARATUS

The heat pipe apparatus and instrumentation were that used in previous work by Naydan [Ref. 4]. A brief description will be provided here; further details are available in Ref. 3.

The heat pipe itself was made from a sixty inch length of two inch outside diameter stainless steel tubing with a wall thickness of 0.020 inches. The ends have been sealed with stainless steel end plates configured with necessary connections for filling and venting. The wick was constructed of four layers of one hundred twenty mesh stainless steel woven cloth held in place by a stainless steel coil spring. The entire apparatus was supported by rigid external frame designed to minimixe heat loss by conduction while permitting rotation of the pipe.

The evaporator section, twelve inches in length, was wrapped with Nichrome ribbon connected to an external DC power supply. Adjacent to the evaporator provision was made for an adiabatic section six inches in length, thus leaving an active condenser length of forty-two inches. The evaporator and adiabatic sections were wrapped with insulation to minimize heat loss.

Thermocouples were installed at two inch intervals along the adiabatic and condenser sections of the pipe. Additionally, thermocouples were installed at ninety degree intervals around the pipe at axial locations eleven and twenty nine inches from the condenser end. Thermocouples also were provided to measure temperatures in the insulation and ambient

temperatures near the condenser. Stainless steel sheathed thermocouples were installed in each end plate, projecting approximately one half inch into the pipe. A Celesco Model PLC Pressure Transducer was used to measure system pressure. The pressure transducer installed at the evaporator end was damaged and not available for use in this experimental work. A known resistance was placed in series with the heater for determination of heater current. All voltages of the thermocouples, pressure transducer and heater were measured using the Hewlett-Packard 2010C Data Acquisition System.

IV. LIQUID CRYSTAL APPLICATION

Reference 4 contains an excellent description of the unique properties of cholesteric liquid crystals and their usefulness in certain temperature-sensing applications. Over a known range of temperature, the liquid crystal will progessively exhibit all colors of the visible spectrum (red to violet) as it is heated through the event temperature range. This phenomenon is reversible and reproducible. By selecting the appropriate cholesteric esters and formulating in the correct proportions, both the width of the event temperature range and its placement on the temperature scale can be controlled. When the liquid crystals are encapsulated in polyvinyl alcohol, a process developed by NCR Corp., the useful life is greatly extended and there is less variation in color due to viewing angle. In the encapsulated form, crystals formulated for different temperatures can be mixed without affecting the color response of each individual formulation.

Commercially available encapsulated liquid crystals are designated by a letter-number combination, e.g., R-41. The letter indicates an event temperature range, in this case approximately $3^{o}C$; the number indicates that the onset of the red color change takes place at $41^{o}C$.

The entire condenser section was spray painted with flat black enamel to provide a suitable surface for viewing the transparent liquid crystals. A mixture of equal parts of encapsulated cholesteric liquid crystals R-41, R-49, and R-56 was

applied to one side of the pipe using a soft camel's hair brush. Four thin coats were applied, allowing two to three hours drying time between coats. No difficulty was encountered in applying the first two coats uniformly, using the crystals in the aqueous slurry form provided by the manufacturer. For the third and fourth coats, the crystal slurry mixture was diluted with an equal volume of distilled water. This successfully countered the tendency of the material to thicken and roll up during application.

V. EXPERIMENTAL PROCEDURE

The evolutions of evacuating the system, loading with methanol and non-condensible gases, and venting the system were accomplished as described by Naydan [Ref. 3]. The one exception was that due to a casualty to the vacuum system, the pipe was only evacuated to approximately ten microns of mercury.

Methanol was used as the working fluid for all data runs. Krypton was used as the heavier gas to provide comparability with Naydan's data. Helium was chosen as the lighter gas because of its availability and overall system compatibility.

The pipe was operated at three different gas load volumes for each of the two gases. The gas loads were selected somewhat arbitrarily. Initially, with the pipe operating at 100 watts nominal input power, sufficient krypton was added to increase the pressure in the pipe about 13.5 pounds per square inch. After the desired data was recorded, the pipe was vented to remove approximately one third of the krypton by reducing system pressure about 4.5 pounds per square inch. The same procedure was followed to produce the third krypton load. Data for calculation of the amount of krypton in the pipe for each run was obtained at steady state ambient conditions as described by Naydan. (See Appendix B for sample calculations.)

After completely evacuating the heat pipe, methanol was loaded and a set of conventional heat pipe data was recorded. Helium was then added to raise system pressure by approximately

22.6 pounds per square inch. After recording desired data, venting was adjusted in an attempt to make second and third helium load volumes comparable to the second and third krypton loads. This was only partially successful as shown in Table I.

TABLE I

HEAT PIPE LOADING

RUN	GAS	METHANOL LOAD (ml)	GAS LOAD (lbm)	GAS PARTIAL PRESSURE AT AMBIENT TEMP. (psi)
1	KRYPTON	172	1.63 x 10-2	11.73
2	KRYPTON	172	1.16 x 10-2	8.35
3	KRYPTON	172	6.07 x 10-3	4.35
4	(None)	168	-	-
5	HELIUM	162	1.39 x 10-3	20.78
6	HELIUM	161	6.37 x 10-4	9.55
7	HELIUM	161	4.02 x 10-4	5.99

At each gas load the heat pipe was operated in both the horizontal and vertical (condenser end up) positions. For each combination of position and gas load except for the second krypton load, the nominal heater input power was varied in twenty five watt increments from 25 to 150 watts. It was decided not to record data beyond 125 watts for the second krypton load since all temperatures were above the range of the liquid crystals applied to the pipe. Evaluation of the data from the first krypton load showed the somewhat anomalous result that system temperatures did not increase appreciably when input power was increased from 125 watts to 150 watts.

Although this phenomenon did not occur with subsequent gas loads, it was decided to record data up to 150 watts even when liquid crystal data was no longer obtainable.

Power lost from the evaporator and adiabatic sections was calculated from temperature drops through the insulation. Net power absorbed by the heat pipe was assumed to be power produced in the heater minus power lost through the insulation. (See Appendix C for sample calculations.)

The angular position of each liquid crystal isotherm was measured at four inch intervals along the condenser section using a template made to match the outer diameter of the pipe. Accuracy was considered to be $\pm 5^{o}$. All measurements were made at the onset of the green color change. No attempt was made to obtain a precise temperature calibration as the relative location and orientation of isotherms were considered to be the important consideration in this work. Comparisons to the installed thermocouples were made, however, during experimental runs. Table II shows the results of the approximate calibration; also included are calibration data for these crystals as reported in Ref. 5.

TABLE II

LIQUID CRYSTAL TEMPERATURE CORRELATION

(Onset of green color change)

LIQUID CRYSTAL	THERMOCOUPLE data (^{o}C)	REF. 5 results (^{o}C)
R-41	41.0 $\pm$1.0	41.0 $\pm$.5
R-49	48.0 $\pm$1.0	47.1 $\pm$.5
R-56	54.5 $\pm$1.5	56.0 $\pm$.5

To ensure that approximately steady state conditions had been reached, data was recorded after the temperature difference between the evaporator end and ambient showed a change of less than one degree Fahrenheit in a fifteen minute period. In no case was data recorded sooner than four and a half hours after a power change.

VI. EXPERIMENTAL RESULTS

Figures 3 and 4 show the temperature variations along the condenser length at one power setting and gas load for each of the two non-condensible gases used. Conventional (methanol only) heat pipe results are shown in Figure 5 for comparison. The temperatures were measured using the installed thermocouples along the top of the pipe in the horizontal position, and along one side of the pipe in the vertical position. Though there are variations in temperature level and gradient, these two plots are quite representative of the type of temperature variations recorded for other conditions. The results in the horizontal position for the krypton load of .00607 lbm agree quite closely with Naydan's results [Ref. 3] at a krypton load of .00565 lbm.

A summary of the data for all experimental conditions is presented in Appendix A. In several of the higher power situations, identified by asterisks in Appendix A, the pipe was apparently operating at or near burnout conditions. In the extreme case, burnout would mean drying of the wick in the evaporator section, unlimited temperature rise, and destruction of the pipe. The specific cause of the high evaporator temperature conditions encountered in this work was not determined.

The isotherms obtained from liquid crystal data are shown in Figures 6 through 17. Although there is some distortion in this two-dimensional presentation, the relevant information

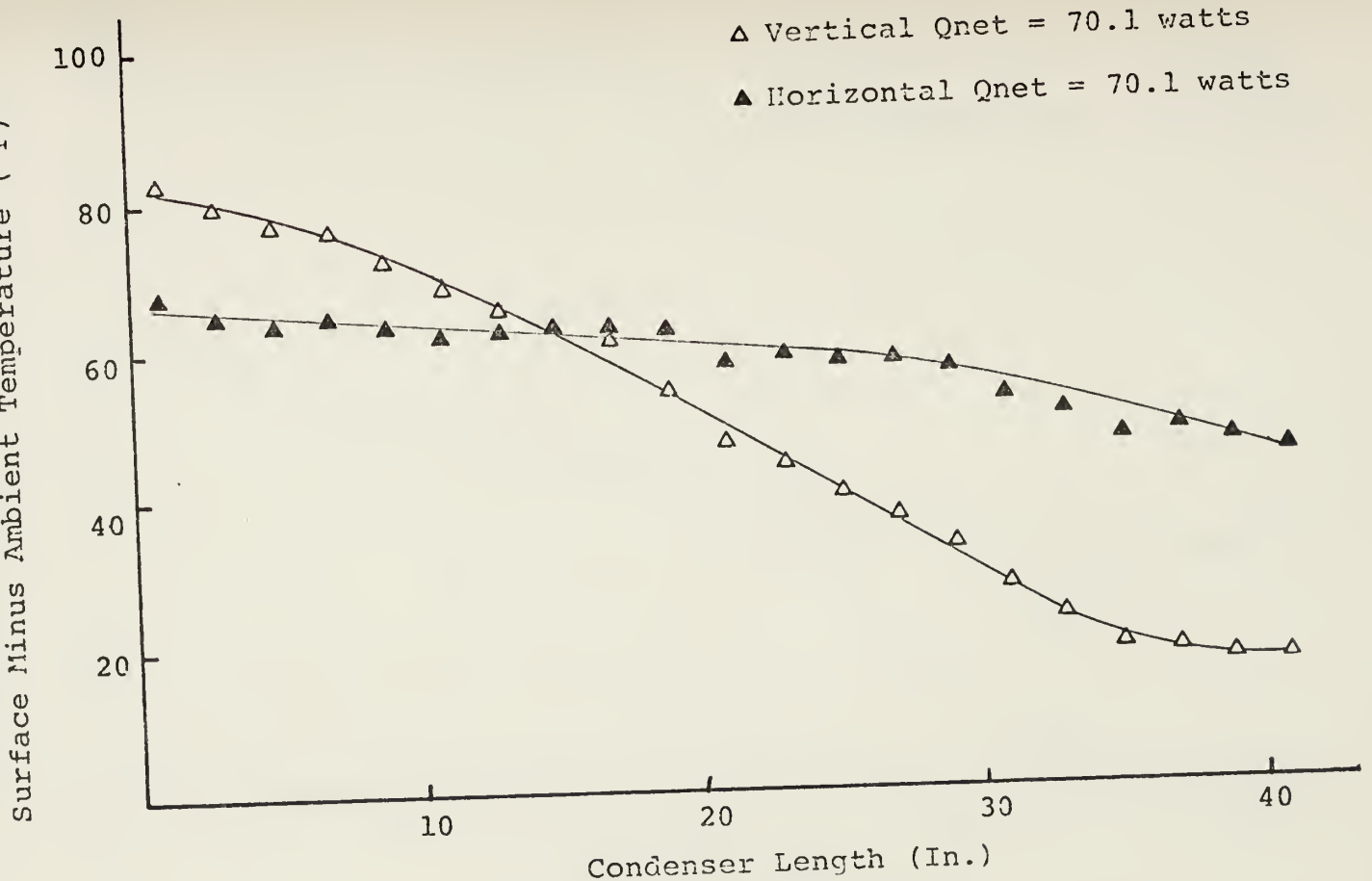

Figure 3. Surface Minus Ambient Temperature vs. Condenser Length - Horizontal and Vertical - .0116 lbm Krypton

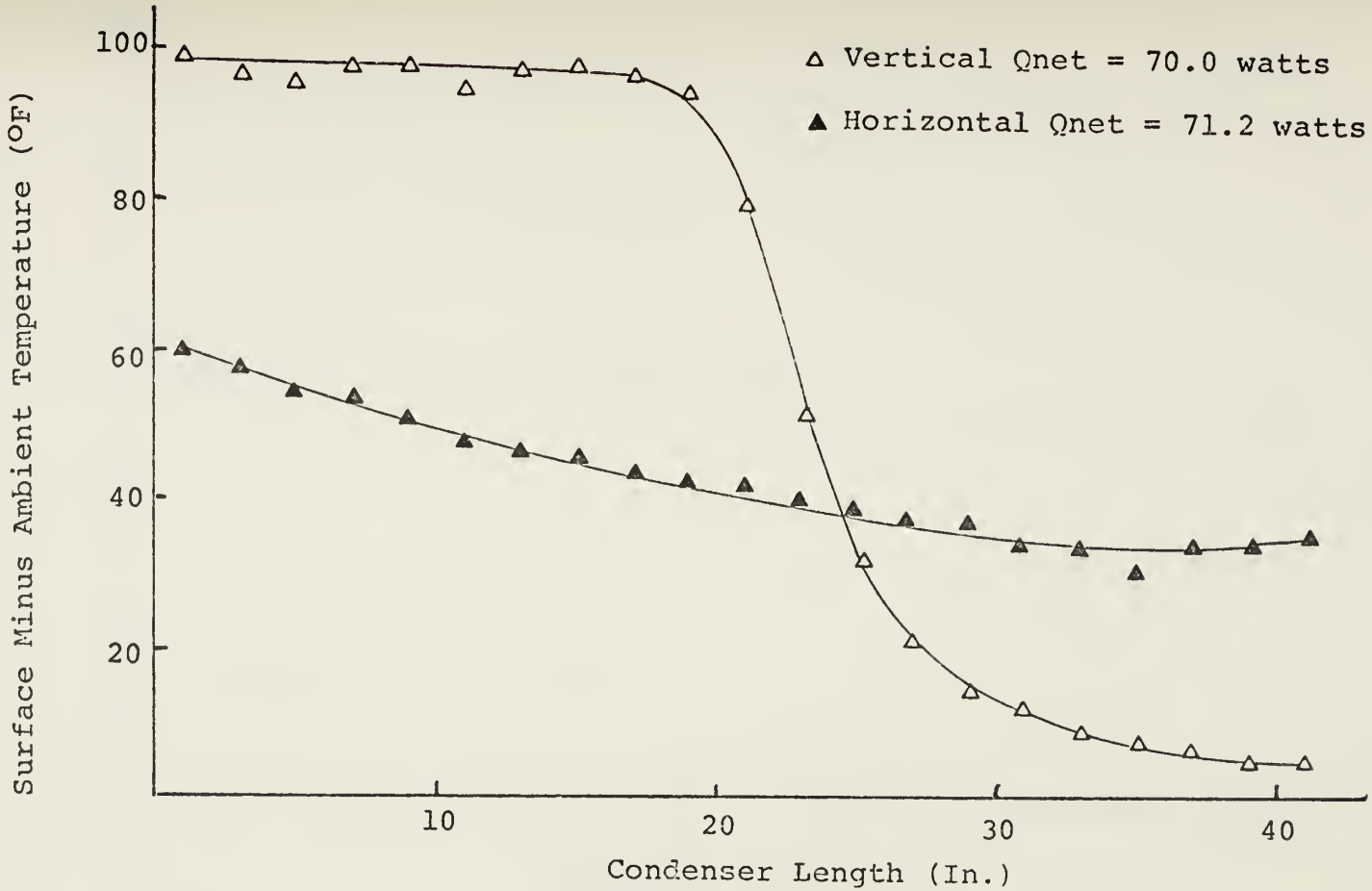

Figure 4. Surface Minus Ambient Temperature vs. Condenser Length - Horizontal and Vertical - .000637 lbm Helium

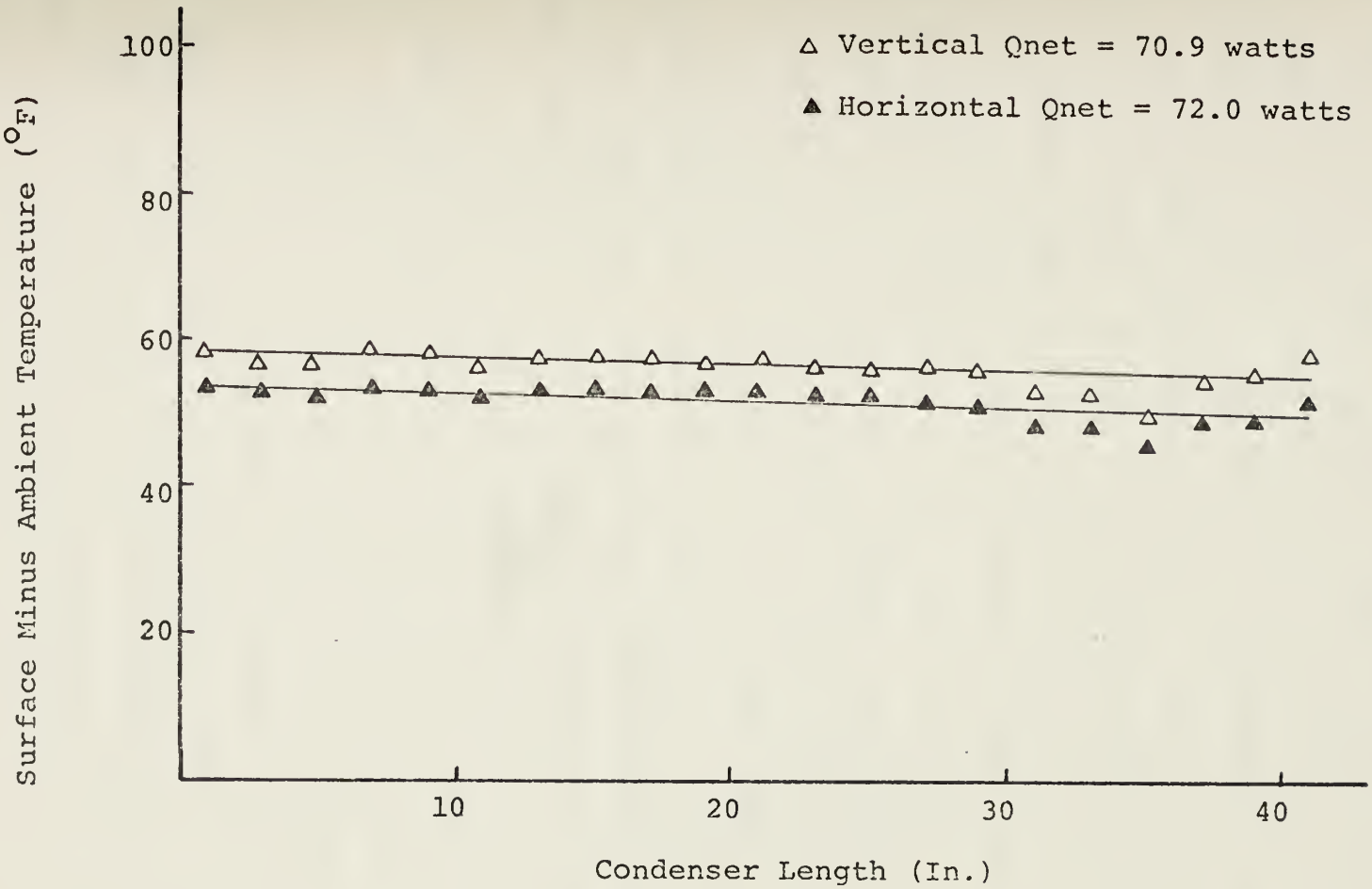

Figure 5. Surface Minus Ambient Temperature vs. Condenser Length - Horizontal and Vertical - Methanol Only

concerning the direction of temperature gradients is retained. Figures 18 through 21 are photographs showing color bands produced by the liquid crystals. These particular photographs were taken at gas loads and power levels slightly different from those for which numerical data is presented. Earlier photographs were not usable because of difficulties encountered with photographic lighting techniques. There is no essential difference, however, in the type of color variation displayed.

The orientation of the isotherms for all of the horizontal settings shows clearly that the non-condensible gas did not form a plug at the condenser end of the heat pipe. Although there was an axial temperature gradient along the pipe, there was a marked temperature gradient perpendicular to the axis. While no quantitative judgements can be made regarding the relative effects of conduction and diffusion across the interface, it seems clear that there was a significant difference in gas concentration from the top to the bottom of the pipe. When the gas was the heavier krypton, the lower temperatures and higher gas concentrations were along the bottom of the pipe. With the lighter helium gas present, the lower temperatures and higher gas concentrations were at the top of the pipe. This leads to a conclusion that the gradient perpendicular to the pipe was the result of gravitational effects.

The temperatures measured by the thermocouples along the top of the pipe provided little indication of the concentration gradients which were present. There was very little difference in the nature of the temperature variation between

the horizontal readings for the two different gases. At higher power levels, the temperature variations had more resemblance to those of the conventional heat pipe than to the gas-loaded variable conductance heat pipe described by the diffuse front theory.

The results with the apparatus in the vertical position were quite different for the two gases. The helium-loaded pipe data showed an axial temperature variation much like the classic diffuse front theory predicts. In the case of the krypton-loaded pipe, temperature decreased continually from adiabatic section to condenser end. In this position the temperature information provided by thermocouples and liquid crystals was quite compatible. It should be noted here that the color bands observed with the pipe in the vertical position when krypton was the non-condensible gas were not stationary. They changed continually with a low amplitude, wave-like motion indicative of a measure of instability.

This data again suggests the influence of gravitational forces. The lighter helium gas readily rose to the upper end of the pipe forming a plug which effectively blocked diffusion of the methanol vapor. Krypton, the heavier gas, was subjected to stronger gravitational forces opposing the momentum imparted by the upward flow of methanol. The result appeared to be a gradually increasing gas concentration, though some methanol vapor did penetrate to the end of the condenser.

The use of liquid crystals proved an effective technique for thermographic mapping. One difficulty was encountered late in the experimental procedure. The color presentation became much less vivid over the section of the pipe approximately twelve inches from the adiabatic section. The only apparent difference was that this section operated at a generally higher temperature than other portions of the condenser. Thus it seems possible that operation at high temperature may have a deleterious effect on encapsulated liquid crystals.

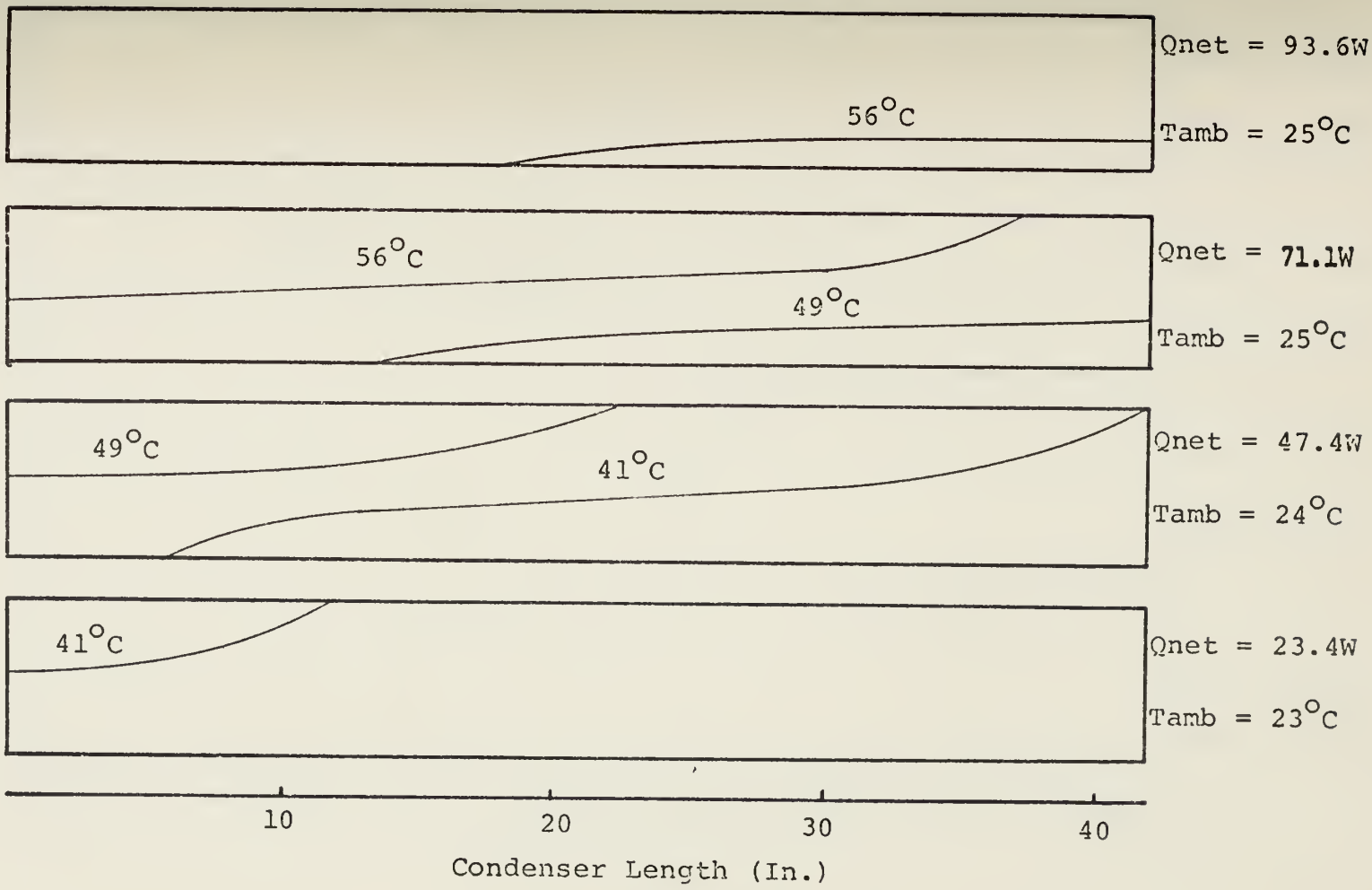

Figure 6. Liquid Crystal Isotherms - Horizontal - .00607 lbm Krypton

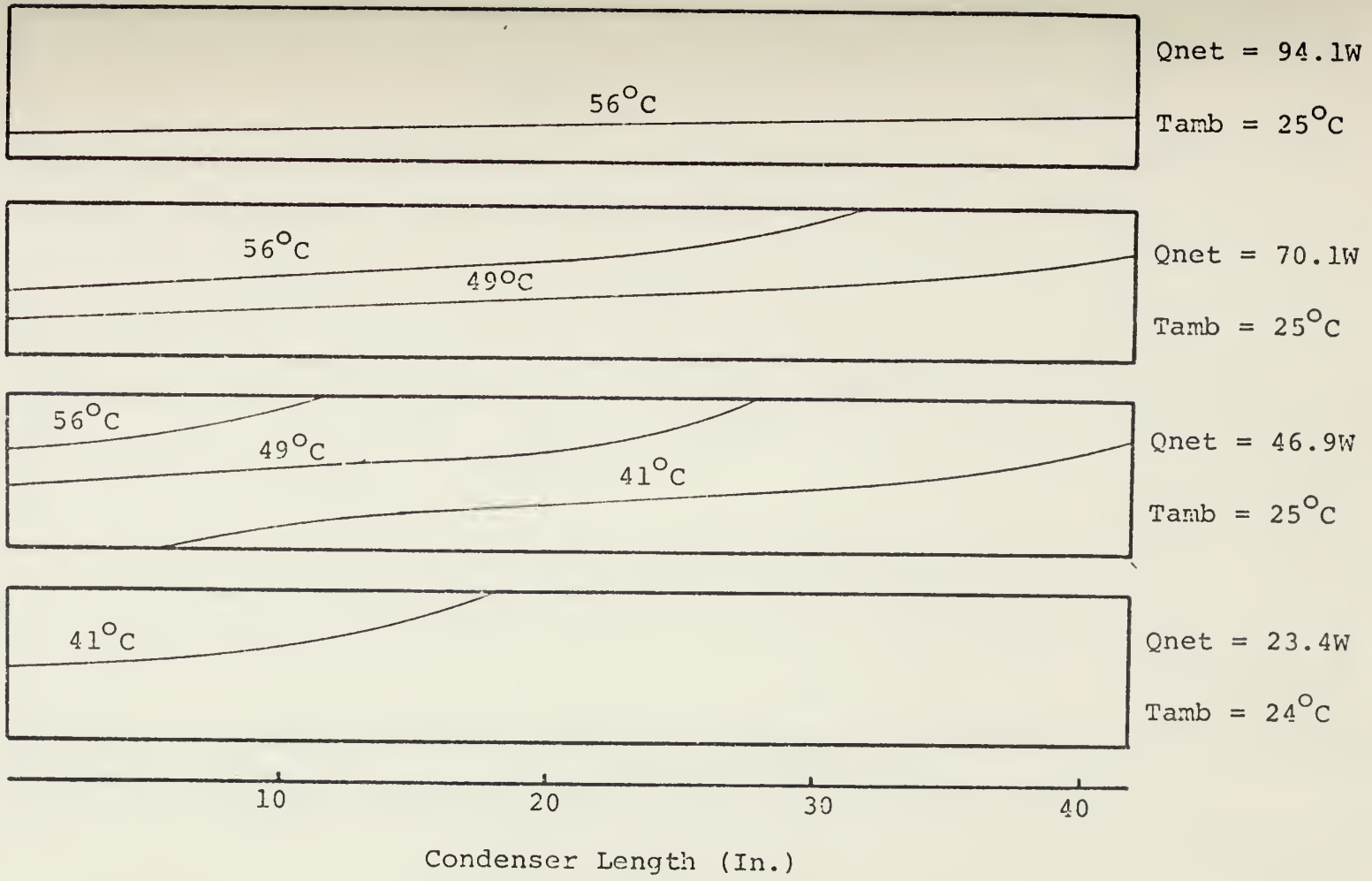

Figure 7. Liquid Crystal Isotherms - Horizontal - .0116 lbm Krypton

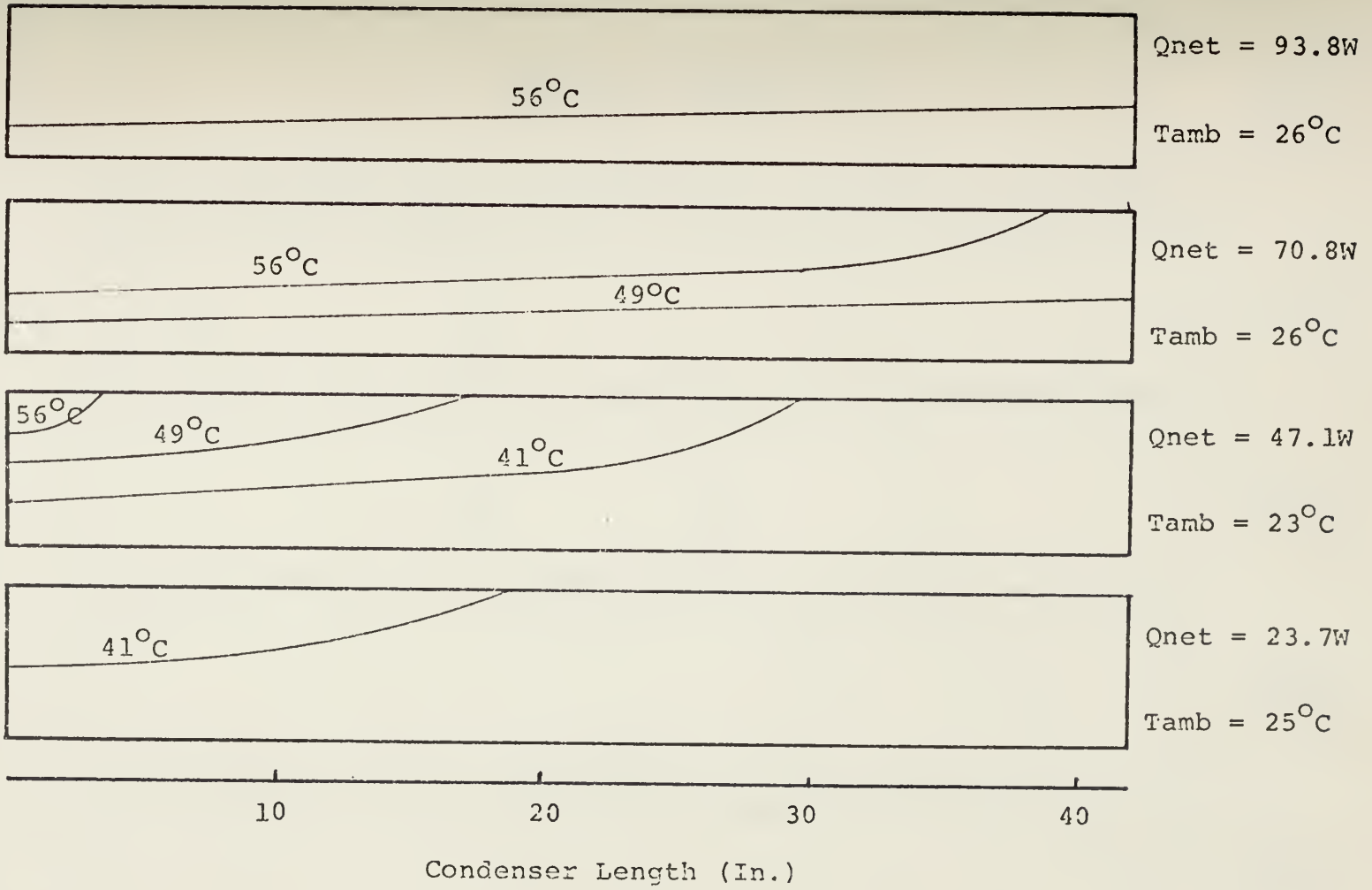

Figure 8. Liquid Crystal Isotherms - Horizontal - .0163 lbm Krypton

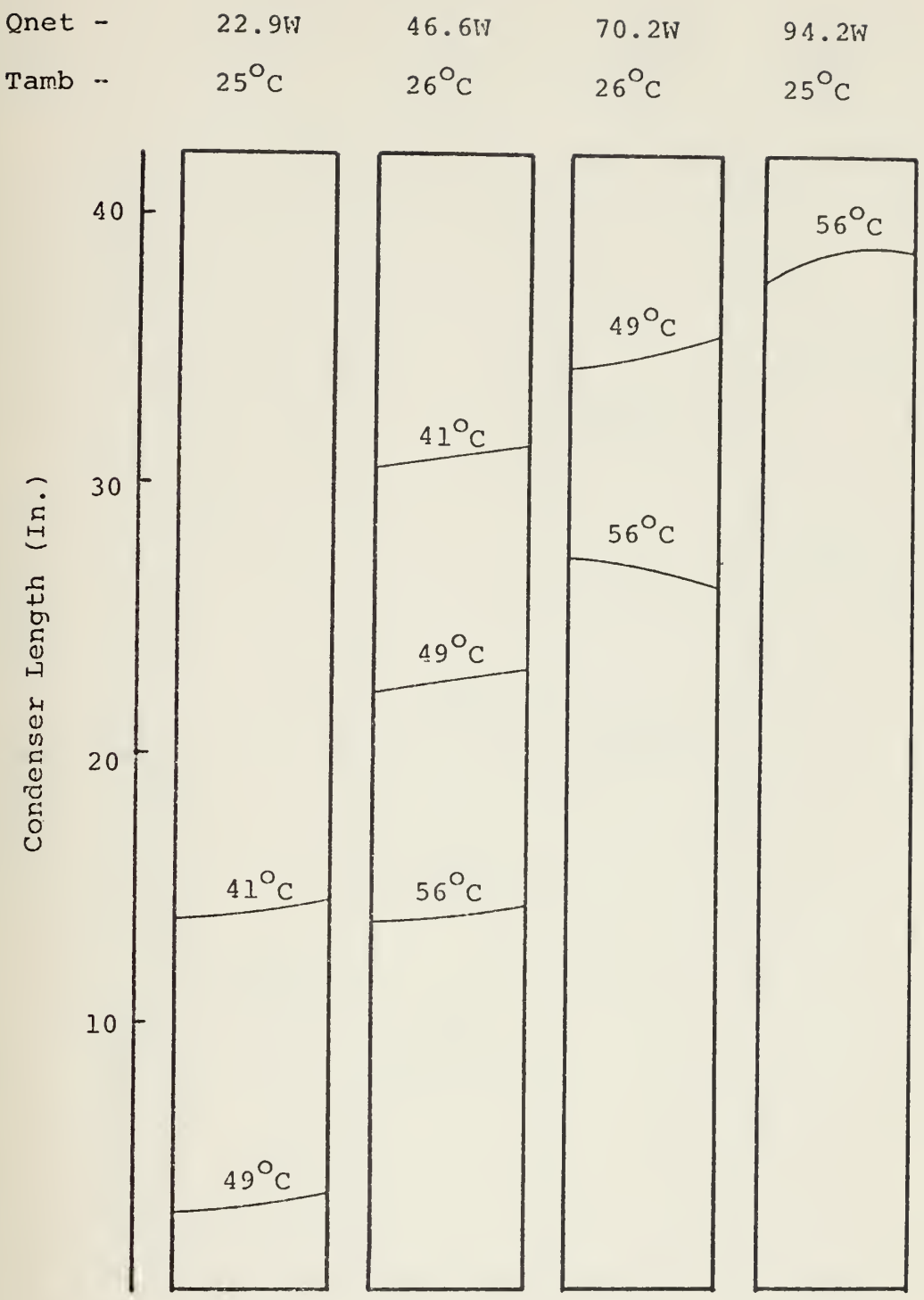

Figure 9. Liquid Crystal Isotherms - Vertical - .00607 lbm Krypton

Qnet -	22.7W	46.4W	70.1W	94.5W
Tamb -	25°C	24°C	25°C	25°C

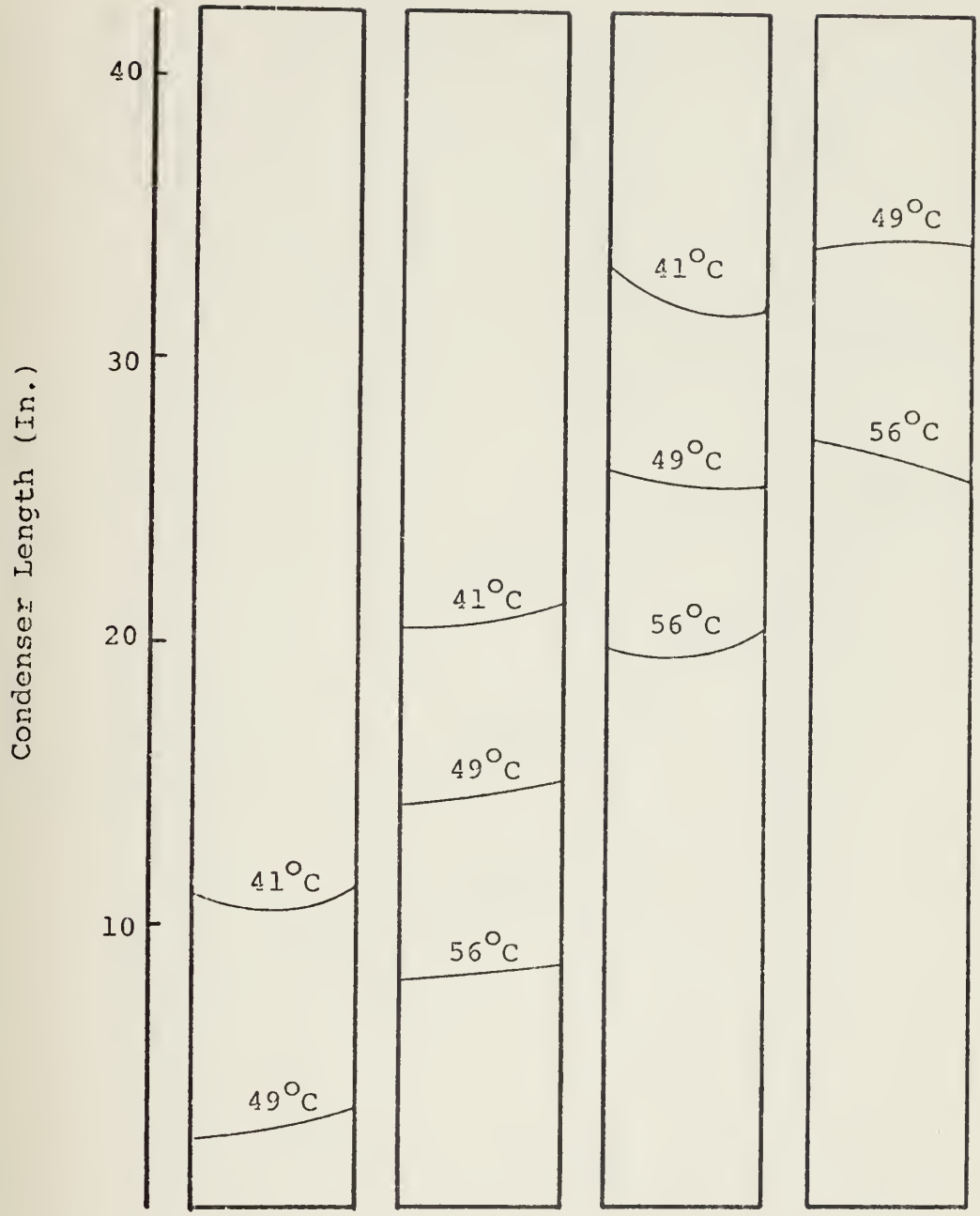

Figure 10. Liquid Crystal Isotherms - Vertical - .0116 lbm Krypton

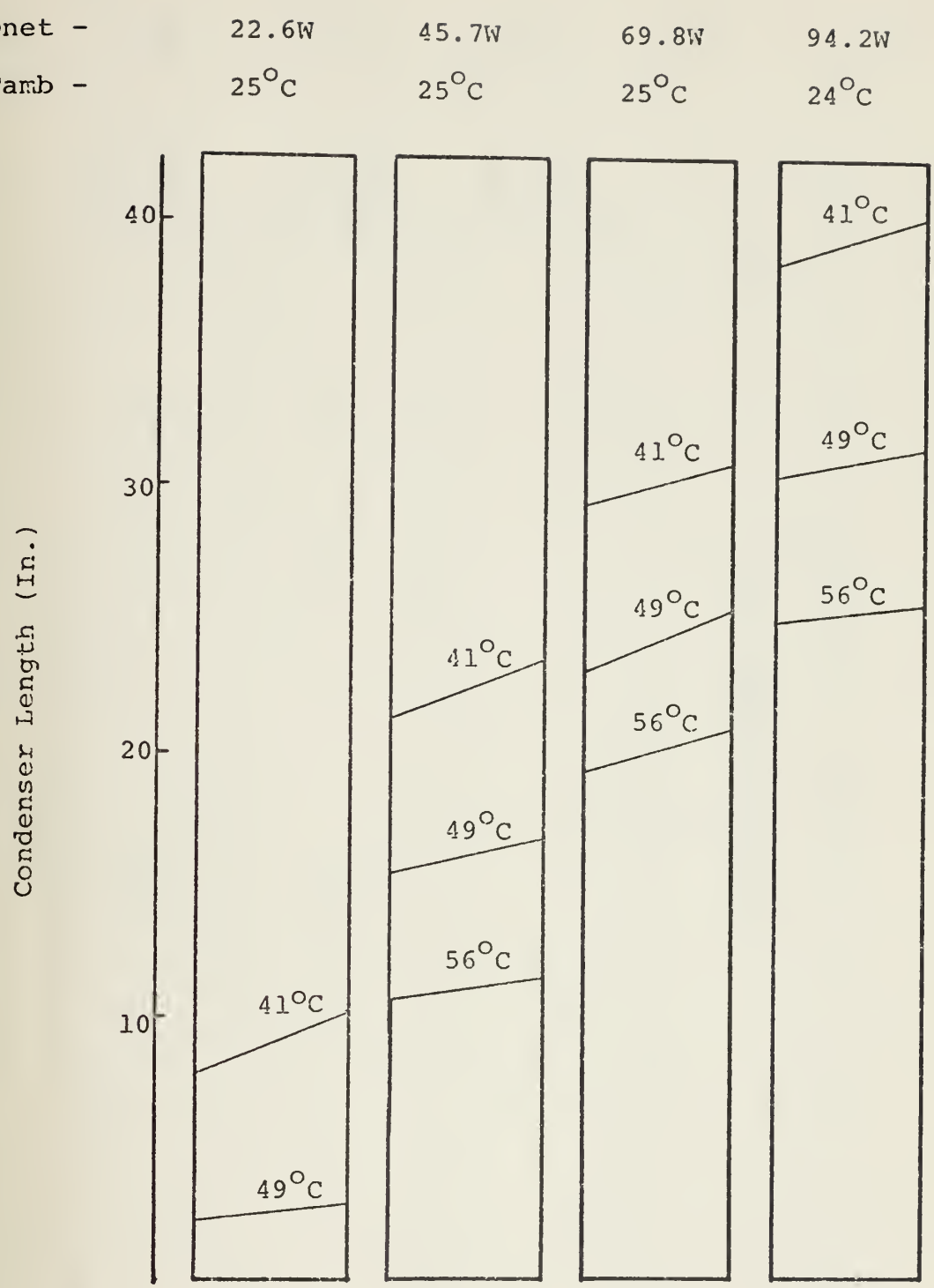

Figure 11. Liquid Crystal Isotherms - Vertical - .0163 lbm Krypton

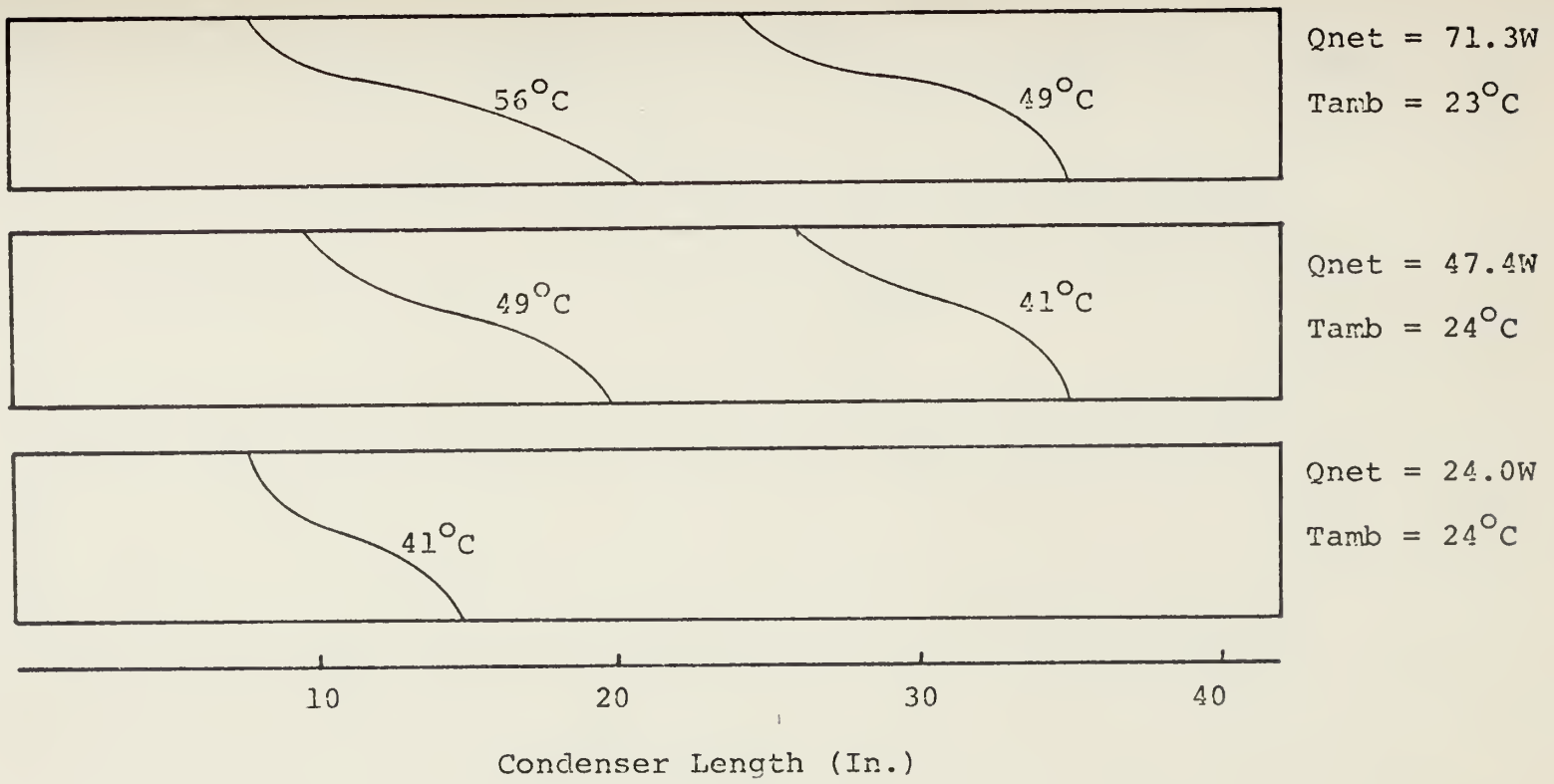

Figure 12. Liquid Crystal Isotherms - Horizontal - .000402 lbm Helium

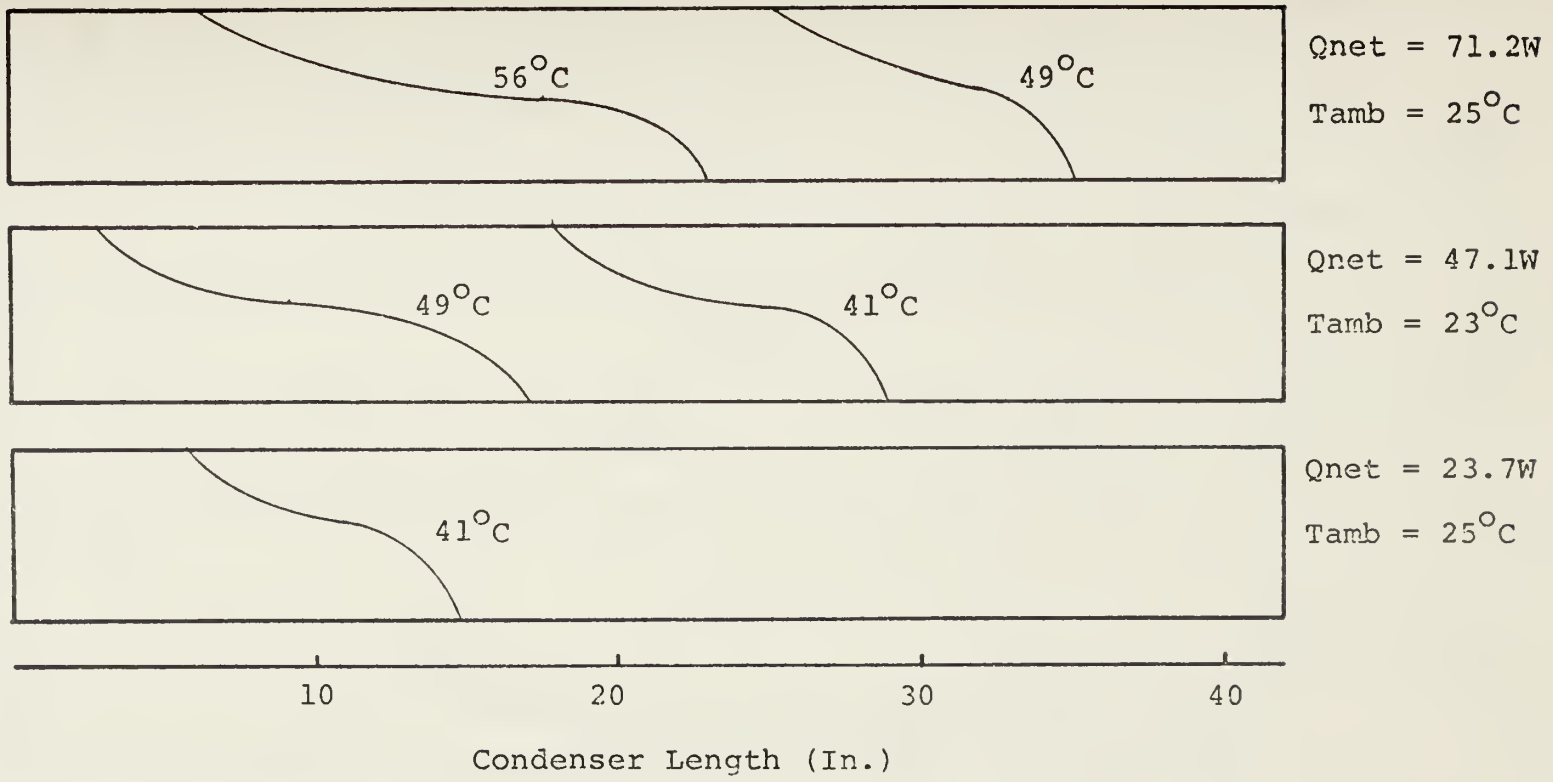

Figure 13. Liquid Crystal Isotherms - Horizontal - .000637 lbm Helium

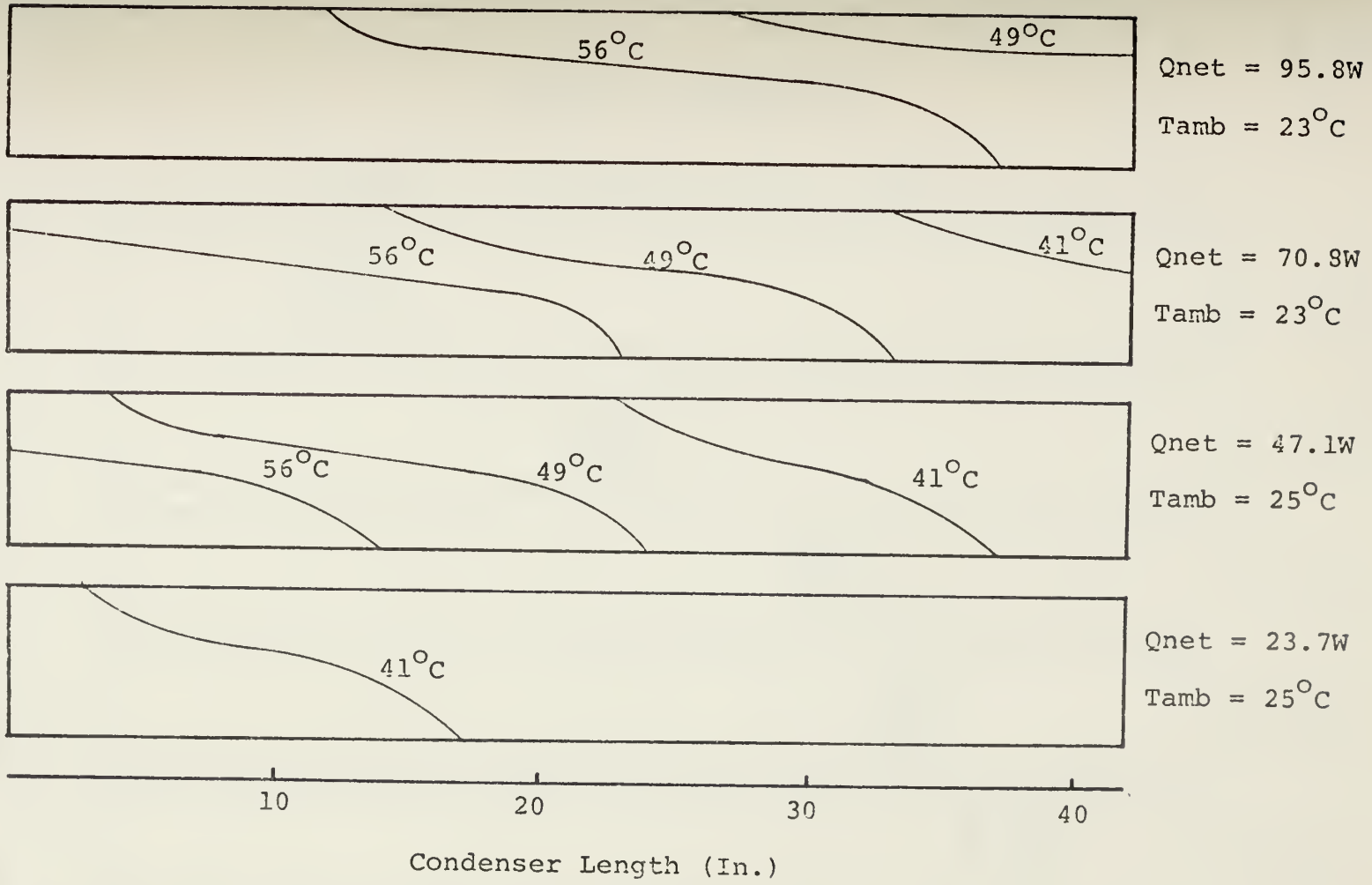

Figure 14. Liquid Crystal Isotherms - Horizontal - .00139 lbm Helium

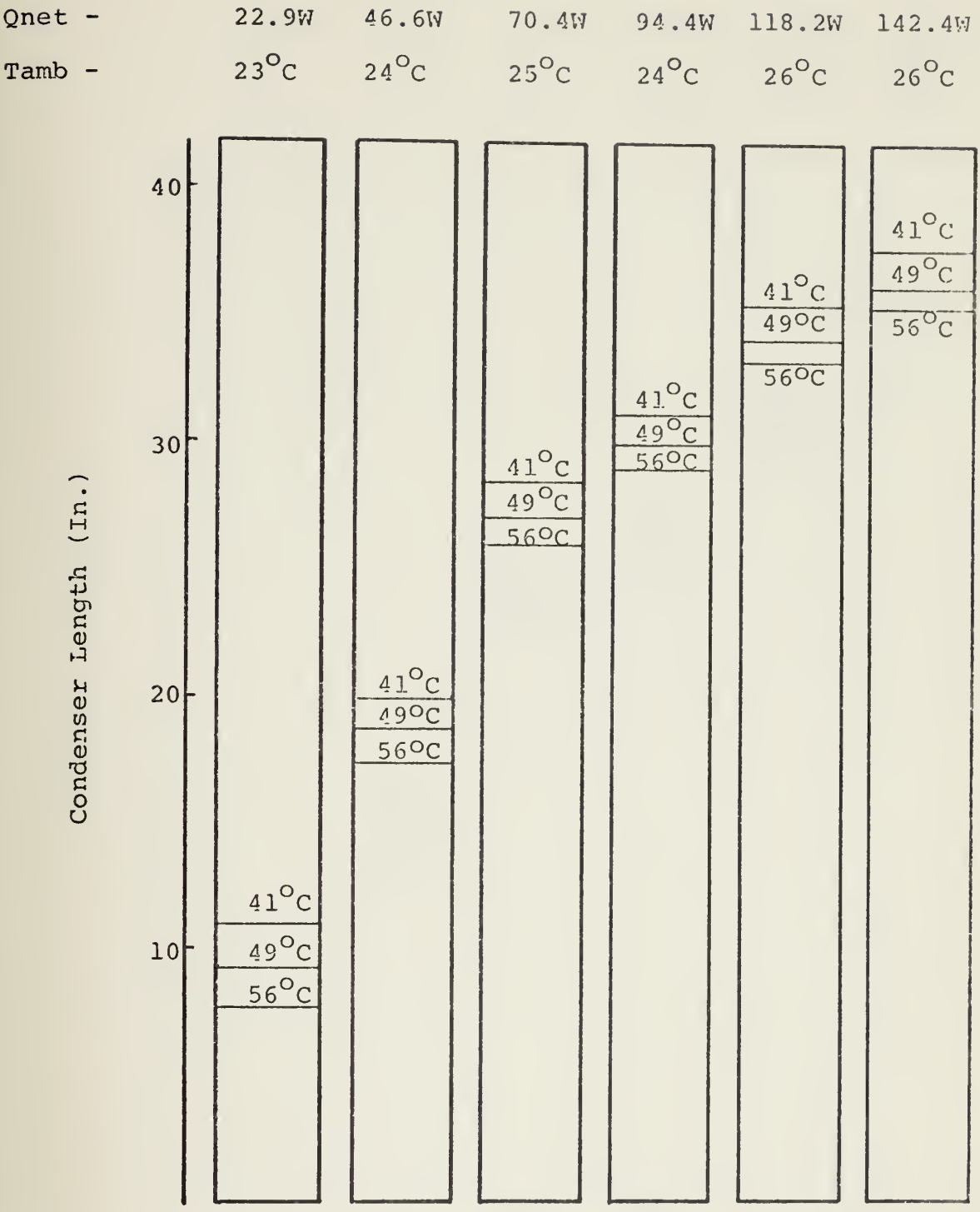

Figure 15. Liquid Crystal Isotherms - Vertical - .000402 lbm Helium

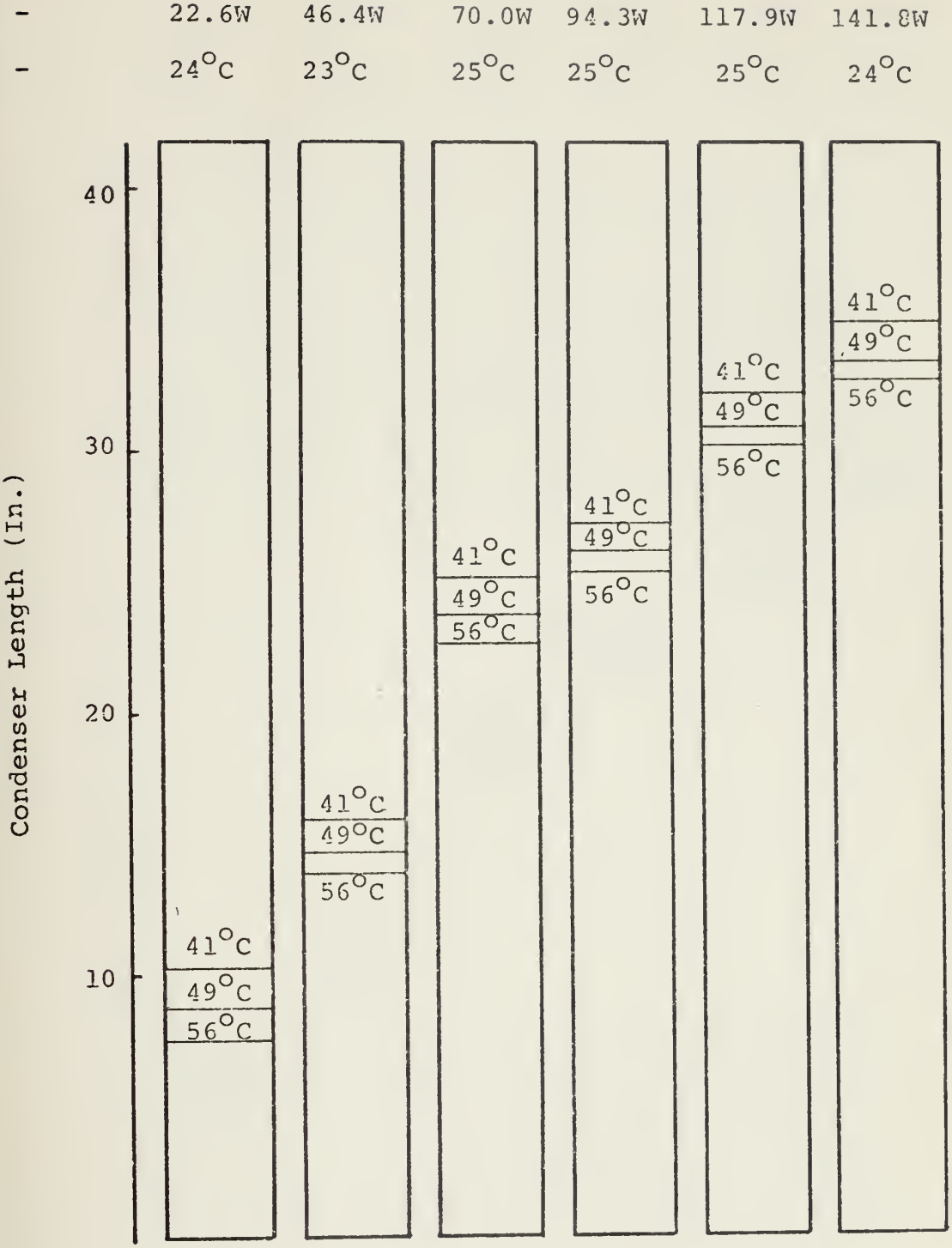

Figure 16. Liquid Crystal Isotherms - Vertical - .000637 lbm Helium

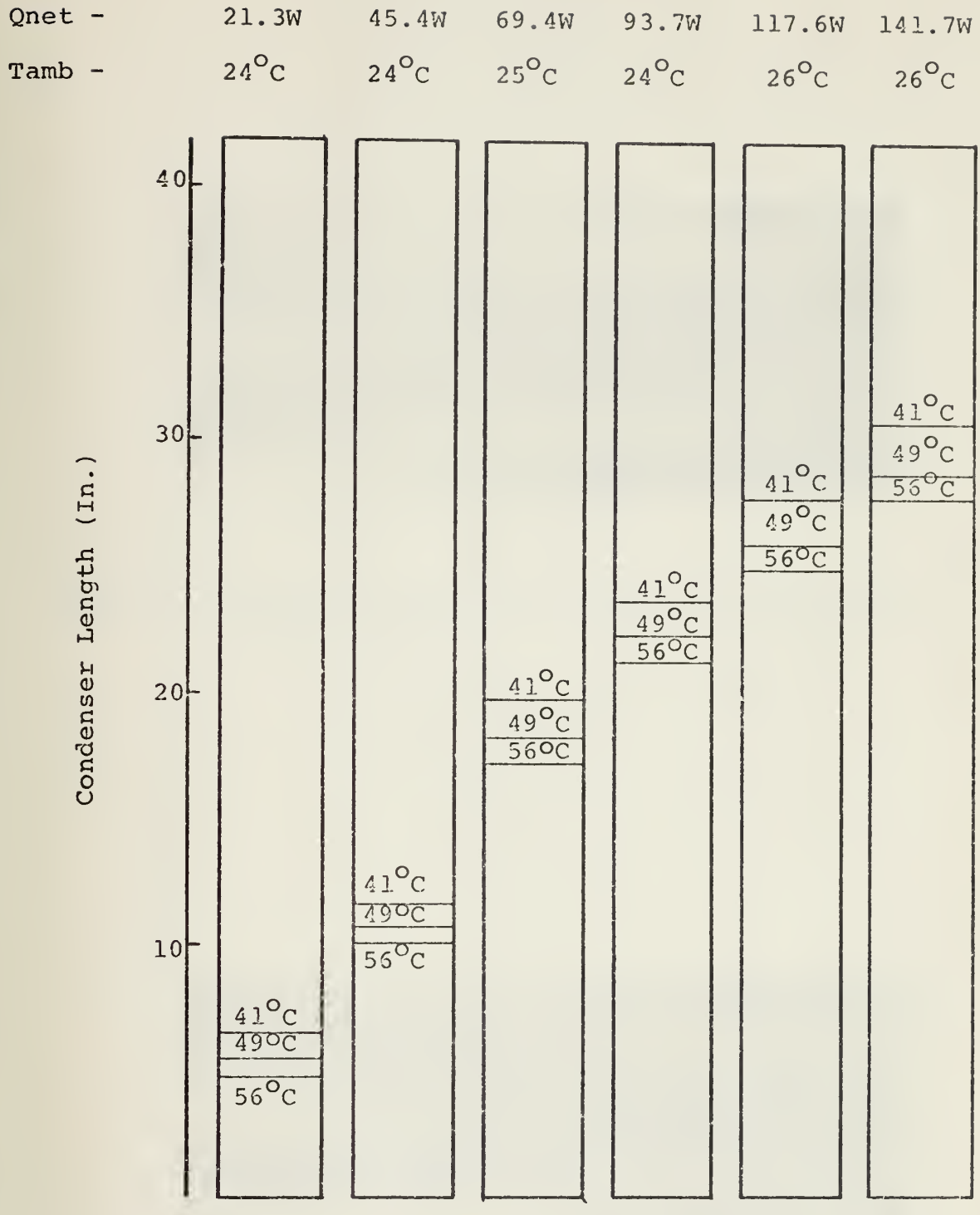

Figure 17. Liquid Crystal Isotherms - Vertical - .00139 lbm Helium

Figure 18. Photograph of Liquid Crystals - Horizontal Krypton Load

Figure 19. Photograph of Liquid Crystals - Horizontal Helium Load

Figure 20. Photograph of Liquid Crystals - Vertical Krypton Load

Figure 21. Photograph of Liquid Crystals - Vertical Helium Load

VII. SUMMARY

The experimental results confirm the existence of a diffuse vapor-gas interface in an operating gas-loaded variable conductance heat pipe. The temperature gradients are indicative of a gas concentration gradient across the interface. The results also show that when the molecular weights of the vapor and gas are significantly different, the gradient and orientation of the interface are appreciably affected by gravitational forces. The diffuse front theory needs to be modified when considering the design of a heat pipe for this combination of factors.

APPENDIX A

SUMMARY OF DATA

Position (Horizontal/ Vertical)	Type of Gas (Krypton/ Helium)	Amount of Gas (lbm,X1000)	Absorbed Power (Watts)	Evaporator Temperature (^{o}F)	Condenser Temperature (^{o}F)	Ambient Temperature (^{o}F)
H	Kr	16.3	23.7	125	87	77
H	Kr	16.3	47.1	138	96	74
H	Kr	16.3	70.8	156	130	79
H	Kr	16.3	93.8	171	145	79
H	Kr	16.3	118.9	201*	161	78
H	Kr	16.3	135.9	245*	181	80
V	Kr	16.3	22.6	151	78	76
V	Kr	16.3	45.7	170	84	77
V	Kr	16.3	69.8	180	94	78
V	Kr	16.3	94.2	189	112	76
V	Kr	16.3	117.4	206	147	79
V	Kr	16.3	140.8	206	144	77
H	Kr	11.6	23.4	122	86	76
H	Kr	11.6	46.9	139	109	77
H	Kr	11.6	70.1	151	125	76
H	Kr	11.6	94.1	173	147	77
H	Kr	11.6	119.7	211*	168	80
V	Kr	11.6	22.7	144	79	76
V	Kr	11.6	46.4	158	84	75

V	Kr	11.6	70.1	171	101	76
V	Kr	11.6	94.5	180	118	77
V	Kr	11.6	118.2	197	150	77
H	Kr	6.07	23.4	116	82	74
H	Kr	6.07	47.4	132	104	75
H	Kr	6.07	71.1	148	130	77
H	Kr	6.07	93.6	168	148	76
H	Kr	6.07	118.3	202*	165	77
H	Kr	6.07	141.4	285*	180	78
V	Kr	6.07	22.9	132	83	76
V	Kr	6.07	46.6	148	100	79
V	Kr	6.07	70.2	161	119	79
V	Kr	6.07	94.2	174	139	78
V	Kr	6.07	118.4	186	157	79
V	Kr	6.07	142.8	199	174	78
H	-	-	24.2	97	96	75
H	-	-	47.9	113	113	76
H	-	-	72.0	132	131	76
H	-	-	96.2	148	148	78
H	-	-	119.8	171	167	78
H	-	-	143.8	189*	180	78
V	-	-	23.8	102	101	78
V	-	-	47.3	121	120	77

V	-	-	70.9	139	138	77
V	-	-	94.4	155	155	77
V	-	-	118.7	170	170	77
V	-	-	142.7	184	184	77
H	He	1.39	23.7	136	81	78
H	He	1.39	47.1	154	101	77
H	He	1.39	70.8	164	113	74
H	He	1.39	95.8	177	134	74
H	He	1.39	119.3	193	160	77
H	He	1.39	143.9	205	177	77
V	He	1.39	21.3	184	75	75
V	He	1.39	45.4	195	76	76
V	He	1.39	69.4	208	79	76
V	He	1.39	93.7	217	79	75
V	He	1.39	117.6	228	85	78
V	He	1.39	141.7	237	88	79
H	He	.637	23.7	132	81	77
H	He	.637	47.1	145	94	74
H	He	.637	71.2	160	120	77
H	He	.637	95.6	174	144	76
H	He	.637	119.1	184	158	76
H	He	.637	143.5	214*	178	78
V	He	.637	22.6	155	76	76

APPENDIX A (Continued)

V	He	.637	46.4	163	74	73
V	He	.637	70.0	180	80	76
V	He	.637	94.3	189	79	76
V	He	.637	117.9	202	84	76
V	He	.637	141.8	213	88	75
H	He	.402	24.0	130	80	76
H	He	.402	47.4	146	102	76
H	He	.402	71.3	157	118	74
H	He	.402	95.0	170	140	76
H	He	.402	120.2	186	163	78
H	He	.402	143.9	198	179	77
V	He	.402	22.9	139	73	73
V	He	.402	46.6	153	76	76
V	He	.402	70.4	169	80	77
V	He	.402	94.4	178	79	76
V	He	.402	118.2	194	89	79
V	He	.402	142.4	205	92	79

*Relatively high evaporator temperature indicative of burnout condition.

APPENDIX B

CALCULATION OF NET ABSORBED POWER

The net power absorbed by the heat pipe is assumed to be approximately equal to the power dissipated in the heater minus the power lost through the insulation. The calculation of the power lost makes use of the temperature difference between thermocouples #94 and #95 positioned at different radial locations in the insulation.

$$q\ (net) = q\ (htr) - q\ (lost)$$

$$q\ (htr) = V_1\ V_2\ /\ R$$

V_1 = voltage drop across heater, volts

V_2 = voltage drop across series resister, volts

R = series resistance (2.0236 ohms)

$$q\ (lost) = \frac{C \ln r_2/r_1}{2\pi K L}\ dT$$

$dT = T_{94} - T_{95}$

r_1 = radius to thermocouple 94 (25/16 inches)

r_2 = radius to thermocouple 95 (25/16 inches)

K = thermal conductivity of insulation

$$\left(.02\ \frac{BTU}{hr\ ft\ ^oF}\right)$$

L = length of insulation (1.1 ft)

C = conversion constant $\left(3.412\ \frac{BTU}{watt\text{-}hr}\right)$

Sample calculation for first data point listed in Appendix A:

$V_1 = 19.58$ volts

$V_2 = 2.64$ volts

$dT = 15.4\ ^{o}F$

$$q\ (net) = \frac{(19.58)\ (2.64)}{2.0236} - \frac{(15.4)(2)(3.14)(.02)(1.1)}{(3.412)\ \ln\ (35.25)}$$

$q\ (net) = 23.7$ watts

Appendix A contains the results for other conditions.

APPENDIX C

CALCULATION OF GAS LOAD

The amount of gas introduced into the pipe was calculated from data obtained at isothermal, ambient conditions.

$$m = \frac{(P_t - P_m)\ V\ M}{R\ T}$$

P_t = total pressure, psia

P_m = methanol partial pressure, psia (saturation data)

V = pipe volume (165 cu. in.)

M = molecular weight of gas

T = pipe temperature, ^{o}R

R = gas constant ($1545 \frac{ft\ \ lbf}{lb\text{-}mole\ ^{o}R}$)

Sample calculation for first krypton load:

P_t = 14.08 psia

T = $536^{o}R$

P_m = 2.35 psia

M = 83.8

$$m = \frac{(14.08 - 2.35)\ (165)(83.8)}{(1545)\ (536)\ (12\ in/ft)}$$

m = .0163 lbm krypton

Other results are listed in Table I.

LIST OF REFERENCES

1. Marcus, B.D., Theory and Design of Variable Conductance Heat Pipes, NASA Contract Report 2018, April 1972.

2. Bienert, W., Heat Pipes for Temperature Control, presented at Intersociety Energy Conversion Engineering Conference, Washington, D.C., 1969.

3. Naydan, T.P., Investigation of a Variable Conductance Heat Pipe, M.S. Thesis, Naval Postgraduate School, 1975.

4. Cooper, T.E., Field, R.J., and Meyer, J.F., "Liquid Crystal Thermography and Its Application to the Study of Convective Heat Transfer," Journal of Heat Transfer, Trans. ASME, v. 97, Series C, No. 3, p. 442-450, August 1975.

5. Naval Postgraduate School Report NPS-59CG73061A, An Analytical Model for Predicting the Daily Temperature Cycle of Container Stored Ordnance, by T.E. Cooper and A. H. Wirzburger, p. 12, 18 June 1973.

INITIAL DISTRIBUTION LIST

		No. Copies
1.	Defense Documentation Center Cameron Station Alexandria, Virginia 22314	2
2.	Library, Code 0212 Naval Postgraduate School Monterey, California 93940	2
3.	Department Chairman, Code 59 Department of Mechanical Engineering Naval Postgraduate School Monterey, California 93940	2
4.	Assoc. Professor M. D. Kelleher, Code 59Kk Department of Mechanical Engineering Naval Postgraduate School Monterey, California 93940	1
5.	CDR William H. Batts, Jr., USN 228 N. Blake Road Norfolk, Virginia 23505	1